AD-A039 904 COLD REGIONS RESEARCH AND ENGINEERING LAB HANOVER N H F/G 8/7
NUMERICAL STUDIES TO AID INTERPRETATION OF AN AIRBORNE VLF RESI--ETC(U)
APR 77 S A ARCONE

UNCLASSIFIED CRREL-77-5 NL

1 OF 1
AD A039 904

END

DATE
FILMED
6-77

CRREL REPORT 77-5

Numerical studies to aid interpretation of an airborne VLF resistivity survey

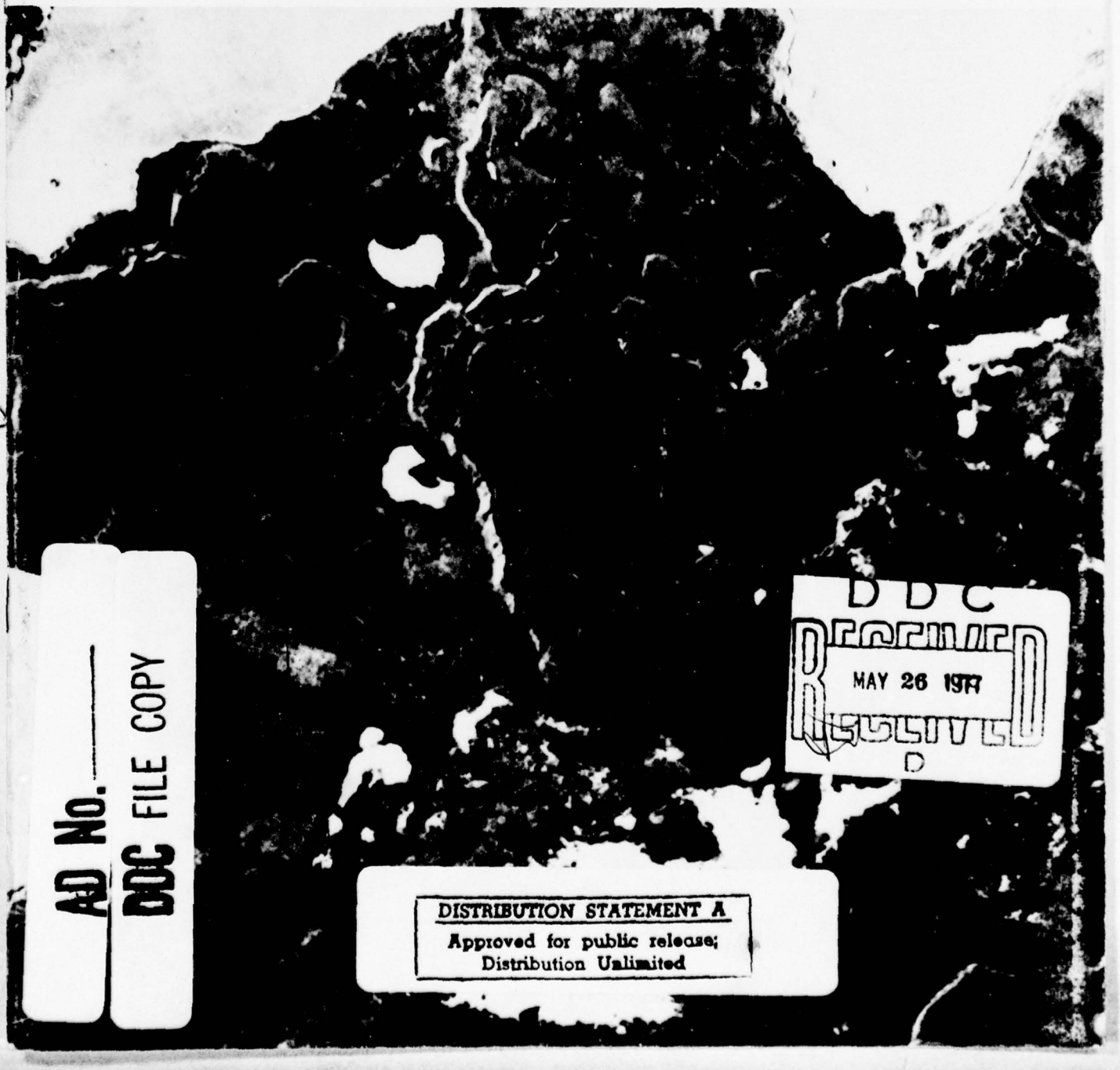

Cover: Aerial view of Tuktoyaktuk Region, Canadian Northwest Territories, over which resistivity surveys were made. (Photograph by Barringer Research, Ltd.)

CRREL Report 77-5

Numerical studies to aid interpretation of an airborne VLF resistivity survey

Steven A. Arcone

April 1977

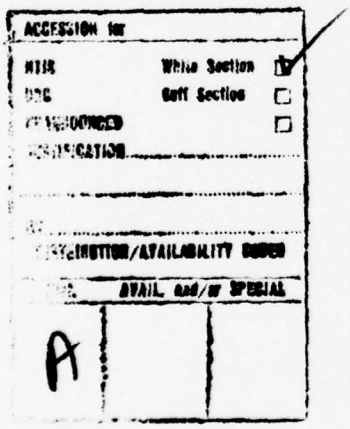

Prepared for
DIRECTORATE OF MILITARY CONSTRUCTION
OFFICE, CHIEF OF ENGINEERS
By
CORPS OF ENGINEERS, U.S. ARMY
COLD REGIONS RESEARCH AND ENGINEERING LABORATORY
HANOVER, NEW HAMPSHIRE

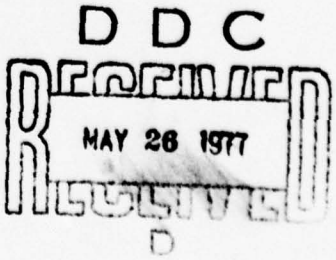

Unclassified

SECURITY CLASSIFICATION OF THIS PAGE *(When Data Entered)*

REPORT DOCUMENTATION PAGE

READ INSTRUCTIONS BEFORE COMPLETING FORM

1. REPORT NUMBER CRREL ~~Report~~ 77-5	2. GOVT ACCESSION NO.
3. RECIPIENT'S CATALOG NUMBER	
4. TITLE *(and Subtitle)* NUMERICAL STUDIES TO AID INTERPRETATION OF AN AIRBORNE VLF RESISTIVITY SURVEY	5. TYPE OF REPORT & PERIOD COVERED
	6. PERFORMING ORG. REPORT NUMBER
7. AUTHOR(s) Steven A. Arcone	8. CONTRACT OR GRANT NUMBER(s)
9. PERFORMING ORGANIZATION NAME AND ADDRESS U.S. Army Cold Regions Research and Engineering Laboratory Hanover, New Hampshire 03755	10. PROGRAM ELEMENT, PROJECT, TASK AREA & WORK UNIT NUMBERS Project 4A762719AT42 Task A2, Work Unit 003
11. CONTROLLING OFFICE NAME AND ADDRESS Directorate of Military Construction Office, Chief of Engineers Washington, D.C. 20314	12. REPORT DATE April 1977
	13. NUMBER OF PAGES 15
14. MONITORING AGENCY NAME & ADDRESS*(if different from Controlling Office)*	15. SECURITY CLASS. *(of this report)* Unclassified
	15a. DECLASSIFICATION/DOWNGRADING SCHEDULE

16. DISTRIBUTION STATEMENT *(of this Report)*

Approved for public release; distribution unlimited.

17. DISTRIBUTION STATEMENT *(of the abstract entered in Block 20, if different from Report)*

18. SUPPLEMENTARY NOTES

037 100

19. KEY WORDS *(Continue on reverse side if necessary and identify by block number)*

Permafrost
Resistivity surveys
Site selection
Subsurface exploration
Wavetilt

20. ABSTRACT *(Continue on reverse side if necessary and identify by block number)*

Airborne resistivity surveys, which use the wavetilt phenomena of radiowaves, are used as a preliminary exploration technique to find suitable areas for either engineering investigations or geologic reconnaissance explorations. Survey results are usually presented as resistivity flight line profiles or as contour maps from which the interpretation or site selection process must be initiated. To aid in this process and provide additional understanding of the correlation between data obtained from airborne and ground surveys, an analysis was performed to determine a very-low-frequency airborne system's response to modelled resistivity anomalies assumed to occur at the surface of an idealized flat earth. Some of the assumptions used to simplify the analysis were based on the results of past surveys. The influences of →

DD FORM 1 JAN 73 1473 EDITION OF 1 NOV 65 IS OBSOLETE

Unclassified

SECURITY CLASSIFICATION OF THIS PAGE *(When Data Entered)*

20. Abstract (cont'd)

survey altitude, anomaly size, and average ground resistivity upon airborne resistivity patterns were analyzed. The results show that the average resistivity of a region plays an important role in suppressing large resistivity contrasts for anomalies of approximately 1-km^2 area. Curves are presented to separate the effects of resistivity contrast and anomaly size, and two examples are given to demonstrate how these curves may be applied to the results of actual surveys.

1 sq. km.

PREFACE

This report was prepared by Steven A. Arcone, Geophysicist, of the Physical Sciences Branch, Research Division, U.S. Army Cold Regions Research and Engineering Laboratory (USA CRREL). The work was performed under Project 4A762719AT42, *Design, Construction and Operations Technology for Cold Regions;* Task A2, *Soils and Foundations Technology for Cold Regions;* Work Unit 003, *Electromagnetic Methods for Subsurface Exploration*.

Technical review of this report was performed by Paul V. Sellmann and Dr. W.D. Hibler III of USA CRREL.

CONTENTS

ILLUSTRATIONS

SUMMARY

The airborne geophysical exploration technique of resistivity surveying by using radiowaves has undergone rapid development in the past few years. This system has been used for locating electrical grounding sites, mapping permafrost, and locating valuable construction materials such as sands and gravels. Survey results are usually contoured into resistivity maps from which sites may be selected for more intensive ground explorations (e.g., drilling).

This research presents the results of a numerical analysis which may aid in the data interpretation process after a VLF resistivity survey has been performed. The simplifying assumptions were that the earth is flat, the very-low-frequency radiowave is planar and incident at a finite grazing angle, and the strength and phase of only the electric field tangential to the earth's surface changes on the surface of the anomaly. The independent variables considered were: 1) contrast in resistivity between the anomaly and the surrounding earth, 2) anomaly size, and 3) survey altitude. Only circular anomalies of radii between 100 and 600 m, a (standard) survey altitude of 75 m, and a uniform phase discrepancy at all points between the field components of interest were considered.

The contoured data from the theoretical study showed the average resistivity of an area to have a large effect on suppressing the measured airborne resistivity contrast for anomalies on the order of 1 km^2. Comparisons of the theoretical analysis with actual field data indicate that the assumptions used were reasonable. Two sets of curves are presented for allowing the effects of anomaly size and resistivity contrast with the adjacent terrain to be separated for two cases: (1) a less resistive (i.e., conductive) anomaly, and (2) a more resistive anomaly. Two examples from past surveys demonstrate the use of these curves in resolving the actual resistivity values and areal dimensions of a ground surface anomaly.

NUMERICAL STUDIES TO AID INTERPRETATION OF AN AIRBORNE VLF RESISTIVITY SURVEY

Steven A. Arcone

INTRODUCTION

Background and objectives

A knowledge of ground resistivity is important to many engineering projects, since it can provide information for determining the locations of: 1) possible sites for providing electrical grounding capability (low-resistivity sites), and 2) possible sites for providing near-surface deposits of sands, gravels and bedrock suitable for construction purposes (usually high-resistivity sites).

To find these locations rapidly and to aid in characterizing the ground conditions of a region rapidly, an airborne geophysical system* was developed (Barringer 1972) and evaluated. This system computes an apparent earth resistivity from the tilt (from vertical) of the electric field vector of low-frequency (200-400 kHz) and very-low-frequency (10-30 kHz) radiowaves. Surveys are usually made along equispaced flight lines and the results are then extrapolated into the form of resistivity contour maps. These maps are commonly superimposed upon a topographic or aerial photomosaic base from which areas of interest can be selected for further ground tests.

The criteria for choosing an area are based on: 1) the proximity of the area to a relevant, planned construction site, 2) the contrast between the resistivities of an anomalous area and a more common area, and 3) the extent of a specified resistivity contour designated as characteristic of the material or conditions sought.

The importance of item 1 is self-evident. Items 2 and 3 are obviously affected by the resistivities of individual locations and the regional extent of the materials present. Item 3 is specifically a method for estimating the actual size of the material present. However, previous field data (Hoekstra et al. 1975) indicated that a great deal of smoothing of ground resistivity information occurs even at minimal flight altitudes of 75 meters. Therefore, an objective was established to develop procedures for better estimating the individual effects of flight altitude, and the areal extent and relative resistivity of an anomalous area.

** The principles, techniques and practice of this system are described in Hoekstra et al. (1974) and will be briefly reviewed in the next section.*

Scope

A VLF plane wave was assumed incident upon a flat earth. A resistivity contrast was established over a circular portion of the surface. The secondary electric fields that resulted from this change were then calculated at a specified survey altitude and superimposed upon the general plane wave field. The resulting field ratios above the anomaly were converted to apparent resistivity values. These values were used to demonstrate the result of the ground-to-air transformation and to determine the approximate size and intensity of a ground anomaly from a knowledge of the ground resistivity values obtained from airborne surveys.

PRINCIPLES OF VLF RESISTIVITY SURVEYING

This section briefly reviews the principles and techniques involved in ground resistivity surveying at very low frequency (VLF). A more complete discussion of the electromagnetic theory involved may be found in books by Wait (1962) and Watt (1967). Surveying technique and results are covered in articles by Hoekstra et al. (1974, 1975), Palacky and Jagodits (1975), McNeill et al. (1973), Frischknecht (1971) and Keller et al. (1970). Discussions of the resistivity of earth materials are presented in Ward (1967), Keller and Frischknecht (1966) and Parkhomenko (1967).

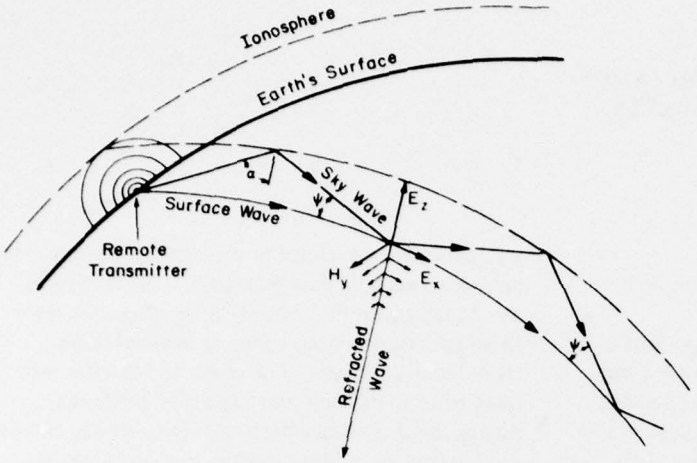

Figure 1. Two radiowave propagation modes in the earth-ionosphere waveguide (see text for explanation of symbols). The electromagnetic field components are characteristic of radiation from a vertical electric dipole or monopole.

Electromagnetic theory

Ideally suited for probing the resistivity structure of the first few hundred feet of the earth's crust are VLF (10-30 kHz) radiowaves. Several VLF transmitters are located throughout the world operating at radiated power levels between 0.1 and 1 MW. At any point on the globe, at least one of these transmitters can be monitored because of this high power and the confinement of the radiation to the earth-ionosphere waveguide.

Within this waveguide, radiation propagates in two important modes, the surface wave mode and the sky wave mode, as illustrated in Figure 1. The *surface wave* mode is so named because the radio wave field strengths attenuate exponentially with height above the earth's surface. The *sky wave* mode is the result of many "hops" or skips off the ionosphere and earth. At the earth's surface the electromagnetic vectors of both these waves are similarly oriented. Referring to the figure, E represents the electric field components and H the magnetic field component in local x, y, z right-hand Cartesian coordinates. α and ψ refer to the incident and grazing angles upon the ionosphere and earth respectively. For sky waves this field configuration results from the vectorial addition of the incident and reflected waves; it is referred to as transverse magnetic and is associated with the vertical electric dipole and monopole types of antennas which are commonly used.

Information about the resistivity of the earth may be obtained by measuring the complex ratio of E_x/E_z (termed the wavetilt W) or of E_x/H_y (termed the surface impedance Z_s). At distances greater than about 800 km, $\psi \rightarrow 0^\circ$ for VLF waves and the radiation is essentially planar. The wavetilt at the surface of a homogeneous earth then can be well approximated as

$$W = \sqrt{i\omega\epsilon_0\rho} \qquad (1)$$

which may also be expressed as

$$W = \sqrt{\omega\epsilon_0\rho}\ \exp(i45^\circ)$$

where $\omega = 2\pi f$ where f is the operating frequency, in Hertz
$\epsilon_0 = 8.85\times10^{-12}$ farads/meter
ρ = resistivity, in ohm-meters
$i = \sqrt{-1}$.

For all simply layered cases, Z_s is simply related to W by the equation

$$Z_s = \sqrt{\mu_0/\epsilon_0}\, W \qquad (2)$$

where $\mu_0 = 4\pi\times10^{-7}$ henrys/meter.

Numerically $Z_s = 377\,W$. Equations 1 and 2 assume that displacement currents are of little consequence at VLF, which is reasonable for most earth materials (for which resistivities are commonly below 10,000 ohm-m).

Resistivity ρ is then obtained by simply inverting eq 1 or 2 and is calculated using the formula

$$\rho = |W|^2/\omega\epsilon_0 \qquad (3)$$

and/or

$$\rho = |Z_s|^2/\omega\mu_0 \qquad (4)$$

which gives the correct value of ground resistivity for a homogeneous earth.

The phase angle of 45° given in eq 1 is diagnostic of homogeneity to at least the depth δ given by the formula

$$\delta = \sqrt{\frac{2\rho}{\omega\mu_0}} \quad . \tag{5}$$

δ is commonly referred to in the literature as the skin depth, the depth at which the refracted wave, shown in Figure 1, attenuates to e^{-1} of its original value of the surface. Its derivation may be found in most textbooks [e.g., Stratton (1941) and Jackson (1962)] on electromagnetic theory. At VLF, δ ranges from about 36 m in a 100-ohm-m material to about 360 m in a 10,000-ohm-m material.

When resistivity layering begins above a depth equal to the skin depth of the upper layer, the magnitude and phase of W (or Z_s) changes according to the resistivities and any layer dimensions involved. A measurement of the ground resistivity is still converted from either W or Z_s as in eq 3 and 4, but only gives some representative value for the composite geoelectric structure. Therefore, ρ must be termed an "apparent" resistivity and is customarily symbolized as ρ_a. Phase, which must always remain between 0° and 90° for vertically stratified homogeneous layers, then becomes diagnostic of the layering present. In general, the following rules apply:

1) Phase angles > 45° indicate that resistivity is decreasing with depth.

2) Phase angles < 45° indicate that resistivity is increasing with depth.

Formulas are available to account for these effects (Wait 1962), but unless more than one frequency (transmitter) is available for measurement, these formulas are of little help in resolving subsurface layering.

Measurement techniques

In the airborne system a pair of horizontal and vertical electric dipoles are used to obtain a measure of the wavetilt magnitude. E_z is selected as the phase reference against which both in-phase and quadrature phase components of E_x may be compared to obtain the total, complex W. However, flight instabilities of the aircraft usually cause the vertical field to couple into the horizontal antenna, thereby producing distortions in the in-phase component of W. Consequently, only the quadrature component is available for computing ground resistivity. This computation then introduces a discrepancy, since it must assume an arbitrary phase angle of 45°, appropriate for only the homogeneous model.

The formula for conversion from wavetilt to apparent resistivity is then

$$\rho_{a_{\text{airborne}}} = \frac{2\,\text{Quad}^2\,(E_x/E_z)}{\omega\epsilon_0} \quad . \tag{6}$$

The relationship between the actual magnitude of the apparent resistivity and that computed from the quadrature wavetilt component is

$$\rho_{a_{\text{airborne}}} = 2\rho_a \sin^2\phi \tag{7}$$

where ϕ is the phase angle. Consequently, there is a system emphasis on resistivity values for materials nearer the earth's surface. This is because $\rho_{a_{\text{airborne}}}$ increases when ϕ is greater than 45° and decreases when it is below 45° in accordance with phase guidelines (1) and (2) on this page.

Ground-based systems are able to measure both phase and amplitude of Z_s. W is not measured on the ground because vegetation strongly disturbs E_z at the earth's surface.

THEORETICAL PROCEDURES

Assumptions

The basic assumptions employed are: 1) the surface is flat, 2) the VLF waves are incident at a finite but small grazing angle ψ, 3) the VLF waves are transverse magnetic and plane, and 4) only E_x changes at the surface of the anomaly.

The final assumption is based on the evidence that where topographic relief is not severe and no highly conductive zones (ore bodies) are present, E_z and H_y remain relatively stable, while only E_x varies sufficiently with resistivity changes to allow a qualitative differentiation of material type based on the computation of apparent resistivity.

The particular cases considered assumed that the homogeneous earth value $\phi = 45°$ does not change over the anomaly. This is not necessary for the computational program to be discussed and any value may be considered for either the earth or the anomaly. The anomaly chosen is represented at the earth's surface as a circular area, although this too is not necessary. It is only chosen for its simplicity. A discontinuous change in the strength of E_x occurs upon encountering the anomaly. Although this is theoretically impossible, it is a reasonable approximation,

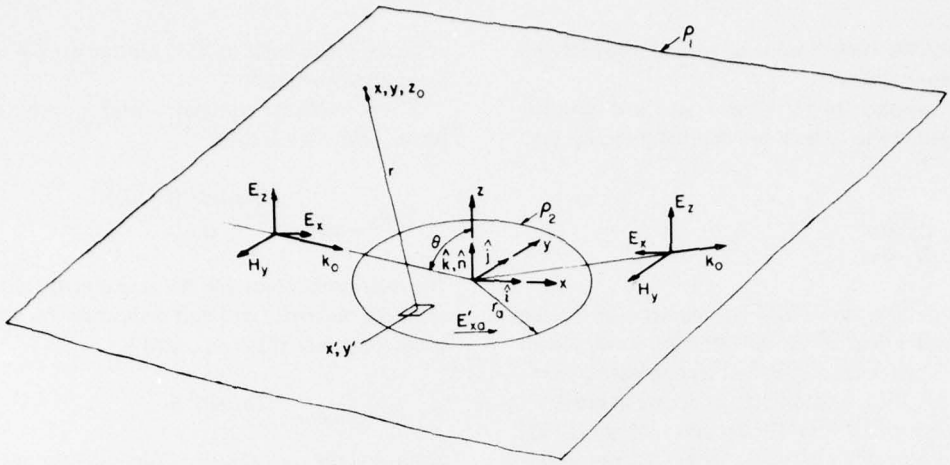

Figure 2. Uniform earth of resistivity ρ_1 containing an anomalous area of resistivity ρ_2. The electromagnetic field vectors refer to the incident (at an angle θ-left) and reflected (right) waves. E'_{xa} is the perturbed electric field on the anomaly. Surface coordinates are primed and spatial coordinates are unprimed. Both coordinate systems have coincident origins. The radius of the circular area is r_a.

since the results of ground surveys discussed in Blomquist (1970) and Hoekstra et al. (1975) have shown that rapid changes in apparent resistivity can occur over distances of only tens of meters.

Mathematical formulations

Far from the transmitter, the electromagnetic fields of a VLF sky wave can be represented at and above the earth's surface as the sum of incident and reflected waves as follows:

$$H_y = H_0 \exp(-ik_0 x \sin\theta)\,[\exp(ik_0 z \cos\theta) + R \exp(-ik_0 z \cos\theta)] \quad (8)$$

$$E_z = H_0 Z_0 \sin\theta \exp(-ik_0 x \sin\theta)\,[\exp(ik_0 z \cos\theta) + R \exp(-ik_0 z \cos\theta)] \quad (9)$$

and

$$E_x = H_0 Z_0 \cos\theta \exp(-ik_0 x \sin\theta)\,[\exp(ik_0 z \cos\theta) - R \exp(ik_0 z \cos\theta)] \quad (10)$$

where H_0 = incident magnetic field strength, in amp-turns/m
θ = complement of ψ in Figure 1
R = reflection coefficient which depends upon θ, ω, and the electrical properties of the earth
$Z_0 = \sqrt{\mu_0/\epsilon_0}$
$k_0 = \omega\sqrt{\mu_0\epsilon_0}$.

A time dependency of exp ($i\omega t$) is assumed. E_x and E_z are expressed in volts/meter and are related to the magnetic field through the vector relation

$$\vec{E} = \frac{1}{i\omega\epsilon_0} \nabla \times \vec{H} \quad (11)$$

where ∇ is the gradient operator and is

$$\nabla = \hat{i}\frac{\partial}{\partial x} + \hat{j}\frac{\partial}{\partial y} + \hat{k}\frac{\partial}{\partial z} \quad (12)$$

where $\hat{i}$, $\hat{j}$, and $\hat{k}$ are unit vectors in the x, y, z directions respectively for a right-hand coordinate system. This system, the unit vectors, and the incident and reflected fields are illustrated in Figure 2. The vector $\vec{k_0}$ in the figure refers to the wave propagation direction and the unit vector $\hat{n}$ is the surface normal.

The effect of a vertical stratification of any number of homogeneous layers of different thicknesses and resistivities is expressed through the reflection coefficient

** These equations satisfy the homogeneous (source-free) Helmholtz wave equations, either $\nabla^2 H + k_0^2 H = 0$ or $\nabla^2 E + k_0^2 E = 0$.*

R. At given values of ω and θ, R may be expressed using the surface impedance Z_s as follows:

$$R = (1 - \beta)/(1 + \beta) \tag{13}$$

where

$$\beta = Z_s/Z_0 \cos\theta. \tag{14}$$

This allows R to be computed from any complex value of Z_s that may be determined experimentally.

Equations 8, 9, and 10 now represent an average, background, plane wave field upon which perturbations resulting from changes in E_x are to be superimposed. Technically, a spatial change in only E_x, without accompanying changes in the other field components, violates the divergence equation $\nabla\vec{E} = 0$ for a source free electromagnetic field. However, this is assumed to be a reasonable approximation based on the experimental evidence referred to in the previous section. Therefore, these local changes are represented as

$$E'_{xa} = (Z_{sa}/Z_s)E'_x \tag{15}$$

where prime = a quantity evaluated at the ground surface
$z = 0$
Z_{sa} = new value of surface impedance
E'_{xa} = new surface value of E_x on the anomalous area.

The net change from the plane wave value in electric field intensity E''_{xa} on the surface of the anomaly is then

$$E''_{xa} = E'_x \left(\frac{Z_{sa}}{Z_s} - 1\right). \tag{16}$$

The secondary fields induced by this local change in E'_x are usually referred to as "scattered" fields. The classical approach to scattering problems involves finding an equivalent set of *surface currents* and *surface charges* to replace the scattering obstacle in question (Harrington 1961). The italicized terms are nomenclatures for the vector and scalar products of the surface normal ($\hat{n}$ in Fig. 2) in question with the associated surface electric and magnetic fields. Since the surface electromagnetic representation of the resistive anomaly has already been assumed, eq 8, 9, 10, and 16 now define these surface fields. For an idealized flat earth, the surface normal coincides with the z axis.

Referring again to Figure 2, the secondary electric fields induced by a specified distribution of $\vec{E}'$ and $\vec{H}'$ over a finite surface area are found from the vector integral equation (Stratton 1941, p. 476)

$$\vec{E} = -\frac{1}{4\pi}\int_{x'}\int_{y'} \left[i\omega\mu_0 (\hat{n}\times\vec{H}')\underline{\Psi} + (\hat{n}\times\vec{E}')\right.$$

$$\left.\times \nabla\underline{\Psi} + (\hat{n}\cdot\vec{E}')\nabla\underline{\Psi}\right] da' \tag{17}$$

where

$$\underline{\Psi} = \exp(-ik_0 r)/r \tag{18}$$

$$r = \sqrt{(x - x')^2 + (y - y')^2 + z^2} \tag{19}$$

da' = an elemental area of integration
x' and y' = surface coordinates for the area of integration in the plane defined by $z = z' = 0$.

The spatial coordinates of the point at which the fields are to be evaluated are defined as x, y, and z. Equation 17 is often referred to as the vector equivalent of Kirchoff's scalar diffraction integral.

Since the only perturbation considered is E''_{xa}, the total airborne electric field is then the sum of the incident, reflected and scattered anomaly fields. Mathematically, this total field is

$$\vec{E} = \hat{i}E_x + \hat{k}E_z - \frac{1}{4\pi}\int_{x'}\int_{y'} (\hat{n}\times\vec{E}''_{xa}) \times \nabla\underline{\Psi}\, da' \tag{20}$$

where E_x and E_z are specified by eq 9 and 10. Carrying out the differentiation, it is found that

$$\vec{E} = \hat{i}\left[E_x - \frac{1}{4\pi}\int_{x'}\int_{y'} z_0 E''_{xa}\frac{\exp(ik_0 r)}{r}\left(\frac{ik_0}{r} + \frac{1}{r^2}\right)da'\right]$$

$$+\hat{k}\left[E_z - \frac{1}{4\pi}\int_{x'}\int_{y'} (x - x')E''_{xa}\frac{\exp(ik_0 r)}{r}\left(\frac{ik_0}{r} + \frac{1}{r^2}\right)da'\right] \tag{21}$$

where z_0 is the specified altitude of surveying. The quadrature value of the wavetilt is then computed from eq 21 and converted to an apparent resistivity using eq 6.

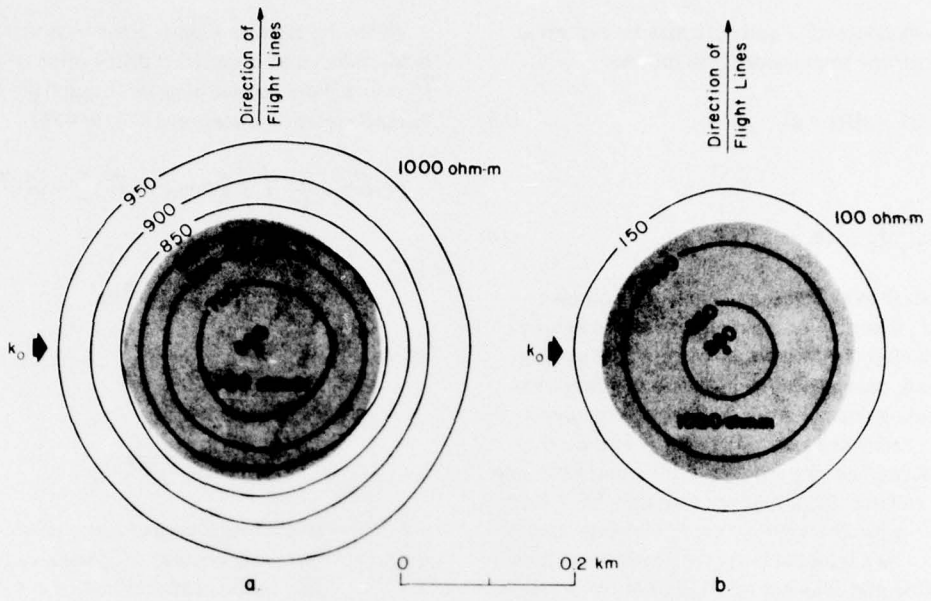

Figure 3. VLF apparent resistivity contours at an altitude of 75 m above a conductive (a) and a resistive (b) circular anomaly. The anomaly radius is 150 m and the incident wave is from the left.

RESULTS

Numerical integrations

Equation 21 was numerically integrated to produce apparent resistivity contours at a standard survey altitude of 75 m above simulated circular anomalies. Each anomaly was 300 m in diameter and the resistivity was greater by a factor of 10 than the background resistivity. The areas of the anomalies were broken into square elements equal to 100 m^2. This size maintained a discrepancy of less than 1.76% between the radial distances from any two points within the element to the airborne point of computation. The calculations used the values $\theta = 87^\circ$ (Watt 1967), frequency = 20 kHz, and assumed that the wave was incident from the left, as was indicated in Figure 2.

The simulated contours are presented in Figure 3 for a conductive (Fig. 3a) and a resistive (Fig. 3b) anomaly. The shaded portions refer to the anomalous surface areas. From the values above the center of the anomalies, it is apparent how influential background resistivity and altitude are upon the anomalous values. Over the conductive anomaly, the value of 660 ohm-m represents a 34% decrease from the apparent resistivity of the background, yet it is still 6.6 times larger than the actual surface value. Over the resistive anomaly, the value of 260 ohm-m represents a 160% increase over the background, yet is only 26% of the actual surface value. At an average flight line spacing of 160 m (present practice), an aircraft should intercept this zone at least within the 700 ohm-m contour of Figure 3a and approximately within the 230 ohm-m contour of Figure 3b.

The slight asymmetry in the x direction results from the inclusion of the term

$$\exp(-ik_0 x' \sin\theta)$$

for the E''_{xa} expression. There is no reason for assuming that this simple plane wave phase dependency maintains itself over such a small anomaly, but the effect is only marginal for the anomaly size considered in this analysis.

In Figures 4a and 4b are plotted curves that permit the effects of resistivity contrast and area size to be separated for the standard survey altitude of 75 m (again, $f = 20$ kHz, $\theta = 87^\circ$, and $\phi = 45^\circ$ for the entire ground surface). In both figures, the background resistivity is given as ρ_1, the anomalous resistivity as ρ_2, and the independent variables are anomaly radius r_a, and resistivity contrast $\beta = \rho_2/\rho_1$. Several computations revealed that these curves could be scaled to within 1% for any resistivity contrast, thereby allowing this type of presentation.

Figure 4a plots the apparent resistivity ρ_a in percentage of ρ_1, above the center of a *conductive* anomaly

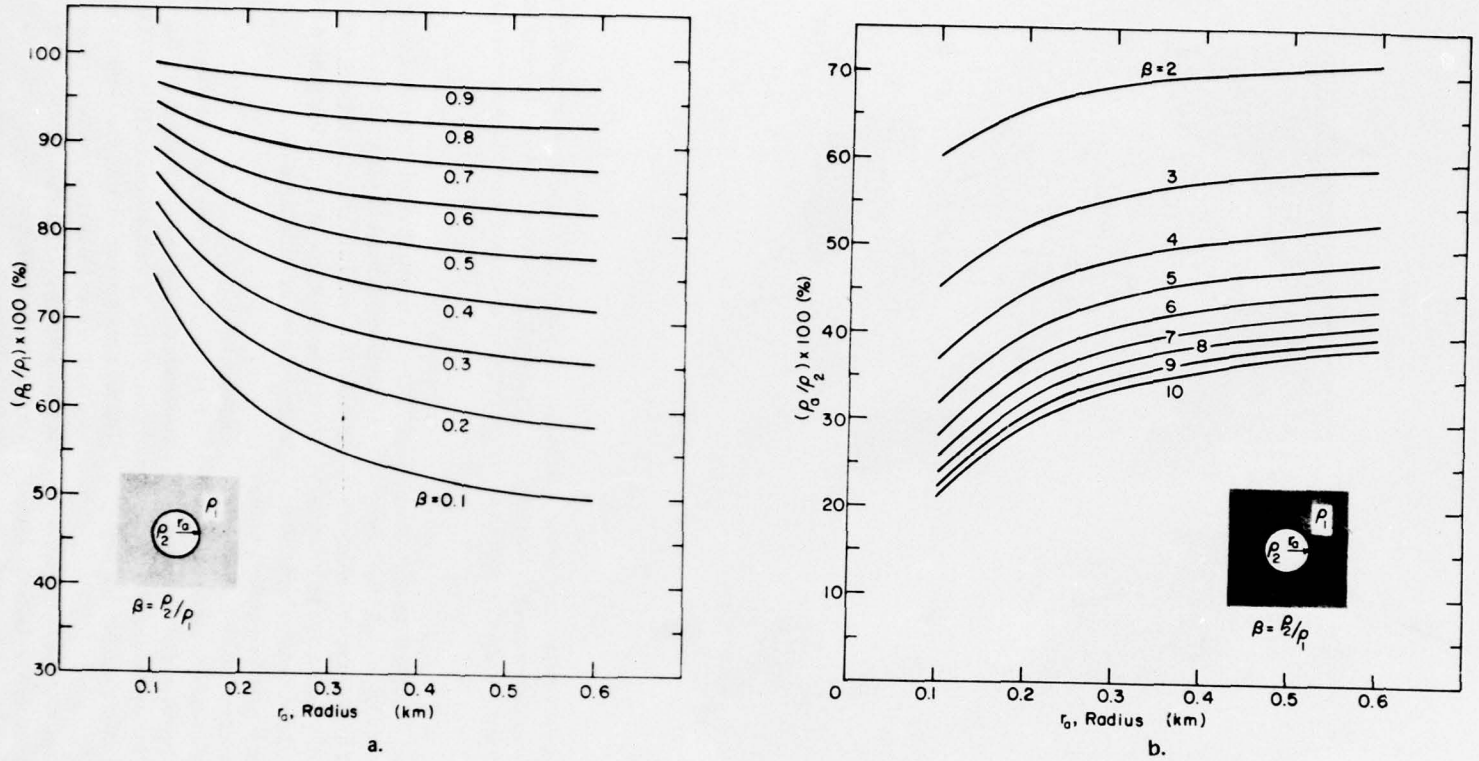

Figure 4. Percentage change of apparent resistivity at 75-m altitude above the center of a resistive anomaly of varying radius r_a. Values are given as a percentage of the background resistivity, ρ_1 (a) and as a percentage of the anomalous resistivity ρ_2(b). The calculations assume f = 20 kHz, $\theta = 87°$, and $\phi = 45°$ at all surface points.

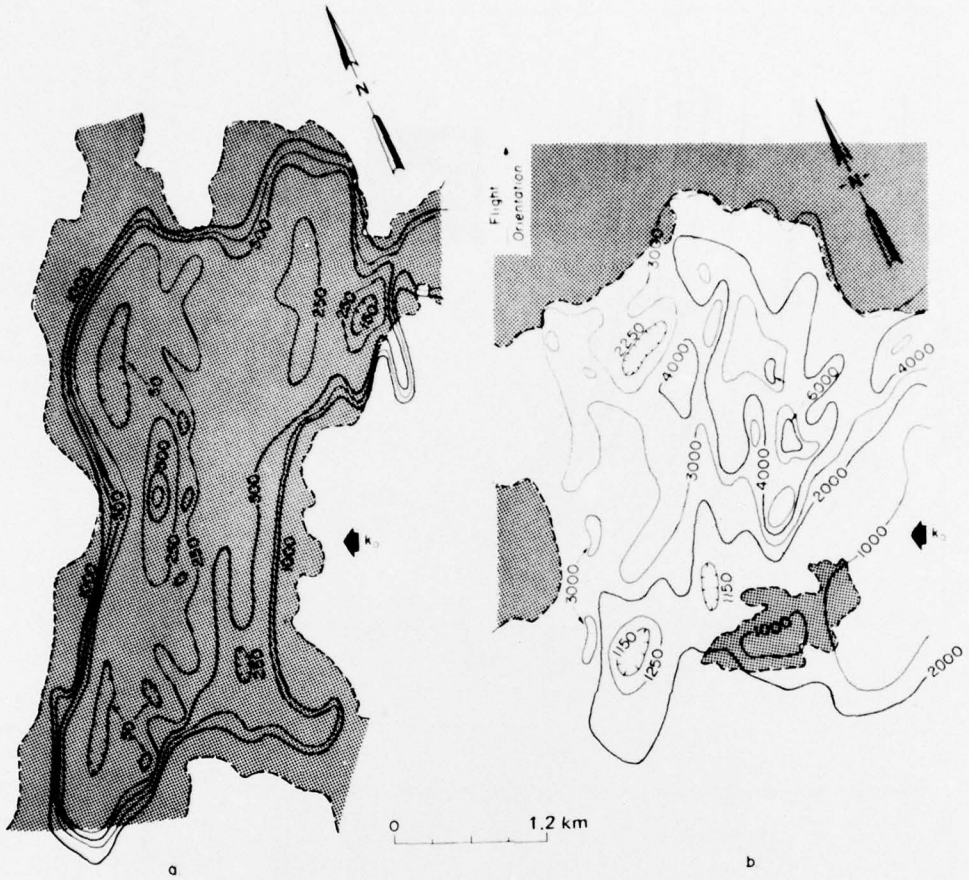

Figure 5. VLF apparent resistivity contours in the Tuktoyaktuk region of the Canadian Northwest Territories above a thawed lake (a) and permafrost (b). Map courtesy of Geological Survey of Canada. Contour values are in ohm-m; shaded portions are areas of deep thaw. (Aerial view of portion of area b is shown on cover.)

($\rho_1 > \rho_2$). Figure 4b plots ρ_a in percentage of ρ_2 above the center of a *resistive* anomaly ($\rho_1 < \rho_2$). Both figures reveal how difficult it is to alter the airborne readings from the background surface value for an anomaly less than 1 km in diameter. The decrease of only 50% at a 75-m altitude revealed in Figure 4a requires a radius of 600 m and a conductive contrast of 10/1. In Figure 4b, a 10/1 increase in surface resistivity for a radius of 600 m results in only a 38% increase at an altitude of 75 m. Both figures imply that beyond the 600-m radius very little change will take place per 100-m increase in radius.

Any further attempts to increase the radius beyond the values given must be limited by two factors. The first is that, as the diameter increases towards an appreciable fraction of a free-space wavelength (15 km at 20 kHz), a model that considers changes in all the field components must be used. The second is that, in order to completely alter the existing background plane wave resistivity value, the integration must be extended over an infinite radius.

Example no. 1

Figure 5 compares the VLF airborne resistivity contours over two different sections of the Tuktoyaktuk region of the Canadian Northwest Territories. The area has little relief and alternates between seasonally thawed lakes over deeper thaw zones (Fig. 5a) and permafrost (Fig. 5b). The airborne differentiation of the thawed zones is apparent. The thawed zones in Figure 5a have an average apparent resistivity of about 250 ohm-m interspersed with some depressions

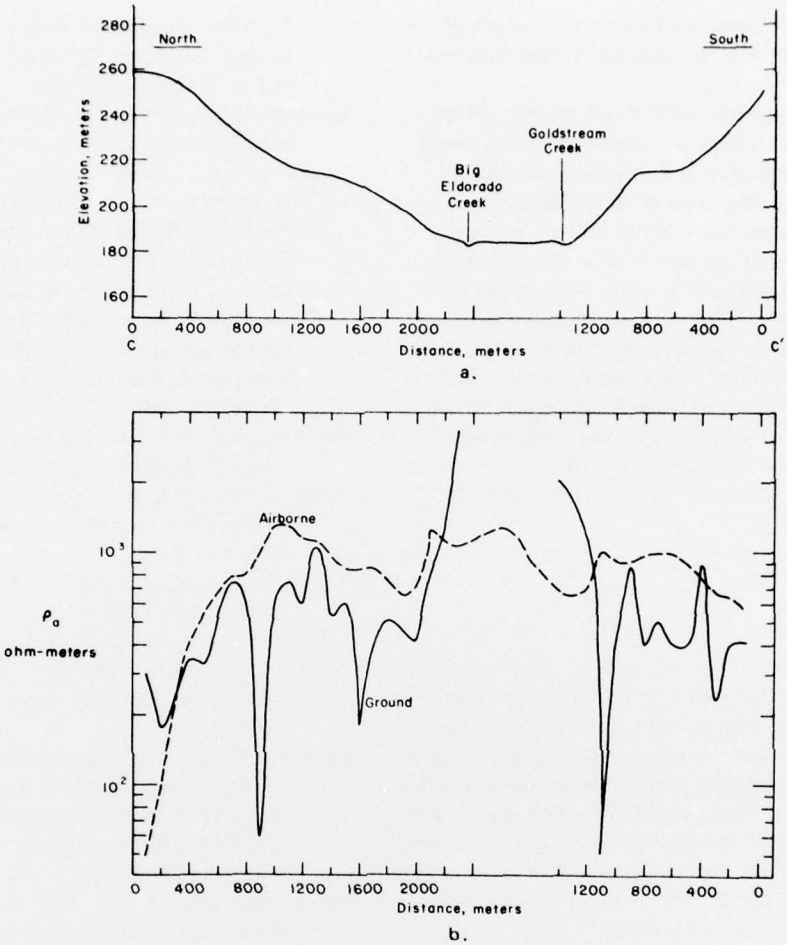

Figure 6. Airborne and ground readings of VLF (18.6 kHz) apparent resistivity (b) across a section of the Goldstream Valley (a) near Fairbanks, Alaska. (After Hoekstra et al. 1975.) The ground readings have been modified according to eq 7.

below 50 ohm-m and one maximum above 600 ohm-m. The permafrost (Fig. 5b) has an average of about 2000-3000 ohm-m with several anomalies above 5000 ohm-m and some depressions near 1000 ohm-m. One of these depressions obviously correlates with the small thaw zone shaded at the lower right of Figure 5b and will be used as an example, since its dimensions can be verified.

This small thaw zone is represented by a closed 1000 ohm-m contour contrasted against an average value of about 2000 ohm-m. This 50% change in value is found at a radius of 600 m on the $\beta = 0.1$ curve of Figure 4a. This value of β implies that the actual resistivity of the anomaly is about 200 ohm-m and the approximate radius is 600, which gives an approximate area of 1.13 km^2. These values compare favorably with the following observations. From Figure 5a the predominant value for a large thaw zone is 250 ohm-m. From the distance scale supplied, the small thaw zone in question is approximately 1.0 km^2 in area.

Example no. 2

A second example is taken from the work of Hoekstra (Hoekstra et al. 1975) in the Goldstream Valley near Fairbanks, Alaska, shown in cross section in Figure 6a. Figure 6b shows the correlation between airborne and ground computations of apparent resistivity taken along a cross section of the valley. The ground readings were modified using eq 7. The detail of the ground readings is lost in the airborne readings, yet both sets of data maintain the same approximate mean level between 800 and 1000 ohm-m. The airborne curve is extrapolated between values recorded

along several flight lines that traversed the length of the valley floor and nearly perpendicular to the cross section given.

The ground data indicate that this central portion of the Goldstream Valley was extremely resistive with quadrature ground values possibly exceeding 3000 ohm-m against a background of about 1000 ohm-m. The width of this portion is about 800 m. A circular approximation [contours presented in Hoekstra's (Hoekstra et al. 1975) article indicated that high resistivities are not continuous along the valley floor] of 400-m radius with a resistivity contrast of 3 is presented in Figure 4b. The figure shows that only about 57% of the true ground value is obtained in the air. From Hoekstra's airborne data, a maximum value of only about 1400 ohm-m is attained by the airborne system over this region, which is 47% of the estimated true level.

CONCLUSIONS

Figures 4a and b present a simple means of recovering ground detail that is lost by altitude in an airborne VLF survey. They also permit preliminary evaluations to be made of the success of an airborne survey in finding conductive or resistive zones covering less than a few square kilometers. Such evaluations would require only the desired value for site resistivity and estimates of the average values for the region considered. Such estimates can now be made rapidly with commercially available and portable VLF field equipment.

LITERATURE CITED

Barringer, A.R. (1972, 1973) Geophysical exploration method using the vertical electric components of a VLF field as a reference. Canadian Patent no. 1,261,732; USA Patent nos. 3,594,633 and 3,763,419.

Blomquist, A. (1970) Equipment for in-situ measurement of the dielectric properties of ground and ice. *Proceedings of the International Meeting on Radio Glaciology, Lyngby, Denmark*, p. 54-70.

Frischknecht, F.C. (1971) Results of some airborne VLF surveys in northern Wisconsin. U.S. Geological Survey, Denver, Colorado.

Geological Survey of Canada (1973) Geophysical survey map of the Tuktoyaktuk Region, Canadian NWT. Open file report no. 220. Map available from the Canadian Geological Survey, Dept. of Energy, Mines and Resources, Ottawa, Canada, N.T.S. Reference 107c/8.

Harrington, R.F. (1961) *Time harmonic electromagnetic fields.* New York: McGraw-Hill.

Hoekstra, P., P.V. Sellmann and A.J. Delaney (1974) Airborne resistivity mapping of permafrost near Fairbanks, Alaska. U.S. Army Cold Regions Research and Engineering Laboratory (USA CRREL) Research Report 324. AD A000694.

Hoekstra, P., P.V. Sellmann and A.J. Delaney (1975) Ground and airborne resistivity surveys of permafrost near Fairbanks, Alaska. *Geophysics*, vol. 40, no. 4, p. 641-656.

Jackson, J.D. (1962) *Classical electrodynamics.* New York: John Wiley and Sons, Inc.

Keller, G.V. and F.C. Frischknecht (1966) *Electrical methods in geophysical prospecting.* New York: Pergamon Press.

Keller, G.V., A.B. Level and F.L. Avsman (1970) Evaluation of airborne electromagnetic surveying for mapping variations in rock strength. Colorado School of Mines, Air Force Cambridge Research Laboratories, Contract Report no. F19628-69-C-0281.

McNeill, J.D., F.L. Jagodits and R.S. Middleton (1973) Theory and application of the E-phase airborne resistivity method. *Proceedings Symposium Exploration Electromagnetic Methods*, University of Toronto, Toronto, Canada.

Palacky, G.J. and F.L. Jagodits (1975) Computer data processing and quantitative interpretation of airborne resistivity surveys. *Geophysics*, vol. 40, no. 5, p. 818-830.

Parkhomenko, E.I. (1967) *Electrical properties of rock.* Translated from Russian by G.V. Keller. New York: Plenum Press.

Stratton, J.A. (1941) *Electromagnetic theory.* New York: McGraw-Hill Book Co., Inc.

Wait, J.R. (1962) *Electromagnetic waves in stratified media.* New York: Pergamon Press.

Ward, S.H. (Ed.) (1967) Article in *Mining Geophysics*, vol. II. The Society of Exploration Geophysicists, Tulsa, Oklahoma.

Watt, A.D. (1967) *VLF radio engineering.* New York: Pergamon Press.